Control Strategy of Active Power Filters Using Multiple Voltage-Source PWM Converters

HIROFUMI AKAGI, AKIRA NABAE, MEMBER, IEEE, AND SATOSHI ATOH

Abstract—**The control strategy of active power filters using switching devices is proposed on the basis of the instantaneous reactive power theory. This aims at excellent compensation characteristics in transient states as well as steady states. The active power filter is developed, of which the power circuit consists of quadruple voltage-source PWM converters. As the result, interesting compensation characteristics were verified experimentally which could not be obtained by the active power filter based on the conventional reactive power theory.**

INTRODUCTION

IN RECENT YEARS, active power filters have been researched and developed to suppress harmonics generated by static power converters and large capacity power apparatus [1]–[5]. Notably, attention has been paid to the active power filter using switching devices such as power transistors, gate-turn-off (GTO) thyristors, and static induction (SI) thyristors, which have made remarkable progress in capacity and switching performance. Various power circuit configurations of the active power filter have been proposed, and the compensation characteristics in steady states have been shown experimentally by Gyugyi and others [6]–[8]. To put the active power filter into practical use, however, it is important to discuss the following:

1) the control strategy, taking into account transient states as well as steady states,
2) the high-efficiency large-capacity converter used as the power circuit,
3) the current control scheme of the converter.

In this paper, the control strategy of the active power filter is proposed on the basis of the instantaneous reactive power theory developed in [9]. This is quite different in principle from the conventional control strategy, thus giving better compensation characteristics in transient states. An experimental active power filter was constructed, of rating 7 kVA (200 V, 20 A). The power circuit consisted of quadruple voltage-source PWM converters using 24 power transistors as the switching devices. The main purpose of the multiple converters was to suppress the harmonics caused by the switching operation without increasing the switching frequency.

The validity of the active power filter was confirmed experimentally. A three-phase thyristor bridge converter of rating 20 kVA was used as an example of harmonic current generators. It was verified that the harmonic current[1] can be fully eliminated not only in steady states, but also in transient states, applying the control strategy proposed in this paper. Through the experiments, the average switching frequency of the power transistors was set to a practical value, i.e., 1.5 ~ 2 kHz, and the total efficiency of the active power filter was 90 ~ 92 percent, including the loss of the multiple transformers.

Paper IPCSD 85-46, approved by the Industrial Drives Committee of the IEEE Industry Applications Society for presentation at the 1985 Industry Applications Society Annual Meeting, Toronto, ON, Canada, October 6–11.

H. Akagi and A. Nabae are with the Technological University of Nagaoka, Nagaoka 949-54, Japan.

S. Atoh is with the Toyo Electric Manufacturing Company, Ltd., Yamato 242, Japan.

IEEE Log Number 8607513.

ACTIVE POWER FILTER SYSTEM

Basic Compensation Principle

Fig. 1 shows a basic compensation principle of active power filters. The compensation objectives of active power filters are the harmonics present in the input currents i_{Lu}, i_{Lv}, and i_{Lw} of the load. Since the compensating currents i_{Cu}, i_{Cv}, and i_{Cw} are controlled so as to eliminate the harmonic currents of the load, the source currents i_{Su}, i_{Sv}, and i_{Sw} become sinusoidal.

Power Circuit Configuration

Fig. 2 shows the active power filter system developed in this paper. The quadruple voltage-source PWM converters are adopted as the power circuit. Note that the primary windings of the four three-phase transformers are connected to each other in series. So, the primary voltage of each transformer is 50 V and the secondary is 100 V. The primary windings of the four transformers can be connected to each other in parallel if the transformers of primary voltage (200 V) and secondary voltage (100 V) are applied. The multiple converters in parallel, however, are less efficient than those in series because of the increase of harmonic currents in each secondary winding and converter.

The converter is a conventional three-phase bridge converter consisting of six power transistors and six power diodes connected back-to-back, as shown in Fig. 3. The turn-off time of the power transistors was about 15 μs and nearly equal to that of large capacity GTO thyristors.

CONTROL STRATEGY BASED ON INSTANTANEOUS REACTIVE POWER THEORY

Instantaneous Reactive Power Theory

Transformation of the phase voltages e_u, e_v, and e_w and the load currents i_{Lu}, i_{Lv}, and i_{Lw} into the $\alpha - \beta$ orthogonal

[1]The term "harmonic" is used in a broad sense to apply to all the distortion components, regardless of their frequency relationship to the fundamental line frequency. Likewise, the term "subharmonic" frequency is taken to mean any frequency below the line frequency, and the term "superharmonic" frequency is taken to mean any frequency above the line frequency [10].

0093-9994/86/0500-0460$01.00

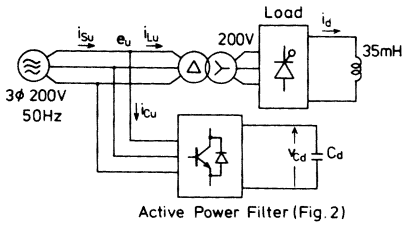

Fig. 1. Basic compensation principle.

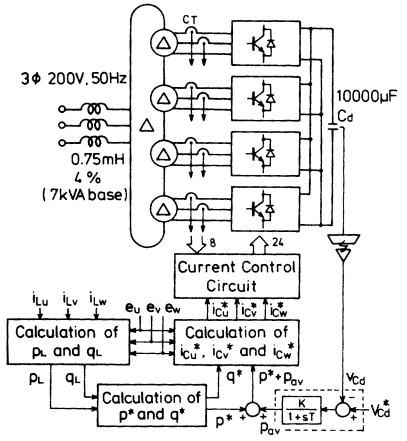

Fig. 2. Active power filter system.

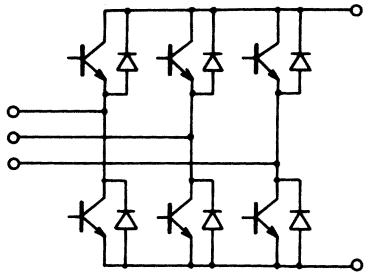

Fig. 3. Three-phase bridge converter.

coordinates gives the following expressions:

$$\begin{bmatrix} e_\alpha \\ e_\beta \end{bmatrix} = \sqrt{\frac{2}{3}} \begin{bmatrix} 1 & -1/2 & -1/2 \\ 0 & \sqrt{3}/2 & -\sqrt{3}/2 \end{bmatrix} \begin{bmatrix} e_u \\ e_v \\ e_w \end{bmatrix} \tag{1}$$

$$\begin{bmatrix} i_{L\alpha} \\ i_{L\beta} \end{bmatrix} = \sqrt{\frac{2}{3}} \begin{bmatrix} 1 & -1/2 & -1/2 \\ 0 & \sqrt{3}/2 & -\sqrt{3}/2 \end{bmatrix} \begin{bmatrix} i_{Lu} \\ i_{Lv} \\ i_{Lw} \end{bmatrix}. \tag{2}$$

According to [9], the instantaneous real power p_L and the instantaneous imaginary power q_L on the load side can be defined as

$$\begin{bmatrix} p_L \\ q_L \end{bmatrix} = \begin{bmatrix} e_\alpha & e_\beta \\ -e_\beta & e_\alpha \end{bmatrix} \begin{bmatrix} i_{L\alpha} \\ i_{L\beta} \end{bmatrix}. \tag{3}$$

Note that the dimension of q_L is not watt, volt·ampere, or var because $e_\alpha \cdot i_\beta$ and $e_\beta \cdot i_\alpha$ are defined by the product of the instantaneous voltage in one phase and the instantaneous current in the other phase. The authors, therefore, introduce to q_L a new dimension IVA, i.e., imaginary volt·ampere.

Equation (3) is changed into

$$\begin{bmatrix} i_{L\alpha} \\ i_{L\beta} \end{bmatrix} = \begin{bmatrix} e_\alpha & e_\beta \\ -e_\beta & e_\alpha \end{bmatrix}^{-1} \begin{bmatrix} p_L \\ q_L \end{bmatrix}. \tag{4}$$

The determinant with respect to e_α and e_β in (4) is not zero.

Let $\bar{p}_L$ and $\tilde{p}_L$ be the dc and ac components of p_L. Likewise, let $\bar{q}_L$ and $\tilde{q}_L$ be the dc and ac components of q_L, respectively. The following relations exist:

$$p_L = \bar{p}_L + \tilde{p}_L \qquad q_L = \bar{q}_L + \tilde{q}_L. \tag{5}$$

From (3)–(5), the α-phase load current $i_{L\alpha}$ is divided into the following components:

$$i_{L\alpha} = \frac{e_\alpha}{e_\alpha^2 + e_\beta^2} \bar{p}_L + \frac{-e_\beta}{e_\alpha^2 + e_\beta^2} \bar{q}_L + \frac{e_\alpha}{e_\alpha^2 + e_\beta^2} \tilde{p}_L + \frac{-e_\beta}{e_\alpha^2 + e_\beta^2} \tilde{q}_L. \tag{6}$$

The physical meaning and the reason for the naming of the instantaneous active and reactive currents are clarified in [9]. Table I shows the relation between the conventional terms concerning "harmonic" currents and frequency components of p_L and q_L. Here, f_i is the line frequency.

Calculation Circuits

In the calculation circuit of p_L and q_L, the calculations of (1)–(3) are performed. In the calculation circuit of the compensating reference currents, the following expression results

$$\begin{bmatrix} i_{Cu}^* \\ i_{Cv}^* \\ i_{Cw}^* \end{bmatrix} = \sqrt{\frac{2}{3}} \begin{bmatrix} 1 & 0 \\ -1/2 & \sqrt{3}/2 \\ -1/2 & -\sqrt{3}/2 \end{bmatrix} \cdot \begin{bmatrix} e_\alpha & e_\beta \\ -e_\beta & e_\alpha \end{bmatrix}^{-1} \begin{bmatrix} p^* + p_{\text{av}} \\ q^* \end{bmatrix} \tag{7}$$

where p_{av} is the instantaneous real power corresponding to the loss of the active power filter, and p^* and q^* are given by

$$p^* = -\tilde{p}_L \qquad q^* = -\tilde{q}_L. \tag{8}$$

Fig. 4 shows the calculation circuit of p^* and q^*. This basically consists of a high-pass filter configuration using a Butterworth low-pass filter. So, this circuit outputs $\tilde{p}_L$ from p_L and $\tilde{q}_L$ from q_L, respectively. The design of the low-pass filter is the most important in the control circuit, because various compensation characteristics are obtained in accordance with the cutoff frequency and order of the low-pass filter, as shown in the experimental results. All the calculation circuits consist of analog multipliers, dividers, and operational amplifiers.

Control Circuit of DC Capacitor Voltage

The control circuit of the dc capacitor voltage is shown in Fig. 2, within the dashed line. The dc capacitor voltage can be controlled by trimming the instantaneous real power p_{av},

TABLE I
RELATION BETWEEN CONVENTIONAL TECHNICAL TERMS AND FREQUENCY COMPONENTS OF p_L AND q_L

Frequency Components of p_L and q_L	Conventional Terms
Equal to 0 (dc)	Active current
	Reactive current
Lower than $2f_i$	Subharmonic current
	Superharmonic current
Equal to $2f_i$	Negative-sequence current
	Superharmonic current (third-order)
Higher than $2f_i$	Superharmonic current

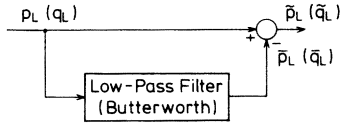

Fig. 4. Calculation circuit of p^* and q^*.

which corresponds to the loss of the active power filter, while the instantaneous imaginary power q^* does not have any effect on the dc capacitor voltage. The control circuit has the negative feedback loop to trim p_{av} automatically, where the time constant T and the gain K determine the response of the control circuit. Note that the active power filter is considered as a harmonic generator rather than a harmonic suppressor when p_{av} is fluctuating. In Fig. 2, the average voltage across the dc capacitor is controlled so as to coincide with the reference voltage V_{Cd}^*, because T is set to 1.5 s and K to 30.

Capacity of the DC Capacitor

To eliminate the harmonics fully, it is necessary to compensate for $\tilde{p}_L$ and $\tilde{q}_L$, as shown in Table I. Elimination of $\tilde{p}_L$, however, causes voltage flucuation of the dc capacitor because $\tilde{p}_L$ is absorbed into the dc capacitor.

Now, let the voltage regulation ϵ be defined by

$$\epsilon = (v_{Cd\,\max} - v_{Cd\,\min})/2\,V_{Cd} \tag{9}$$

where V_{Cd} is the average voltage of v_{Cd}, and nearly equal to V_{Cd}^*. Considering that $\tilde{p}_L$ is sinusoidal, i.e.,

$$\tilde{p}_L = P_m \cdot \sin\ \omega t,$$

the voltage regulation is derived as follows:

$$\epsilon = P_m/\omega \cdot C_d \cdot V_{Cd}^2. \tag{10}$$

From (10) it is evident that the lower the frequency of $\tilde{p}_L$, the larger the capacity of the dc capacitor to suppress the voltage fluctuation.

CURRENT CONTROL SCHEME OF MULTIPLE VOLTAGE-SOURCE PWM CONVERTERS

The current control scheme of the multiple voltage-source PWM converters must provide the following:

1) quick current controllability,
2) suppression of the harmonics caused by the switching operation, and
3) equalization of the average switching frequency of each PWM converter.

Basic Current Control Schemes

Generally, there are two basic schemes for PWM current control. The first, as shown in Fig. 5(a), determines the PWM switching sequence by means of comparing the current error signal amplified by the gain K_p with a triangular carrier signal. Thus the switching frequency of the power transistors is equal to the frequency of the triangular carrier signal. When the scheme is applied to the multiple PWM converters, the phase of each carrier signal is shifted as usual. For example, the phase is shifted by $\pi/2$ in the case of quadruple converters. The harmonic currents, therefore, are reduced as if the switching frequency were increased. However, the error between the reference current and the actual current is produced because of the finite gain.

The second scheme, shown in Fig. 5(b), consists of imposing a deadband or hysteresis around the reference current. Whenever the actual current tries to leave the band, the appropriate device is switched on (off), forcing the current to return to the band. This enables quick current controllability, but it is difficult in requirements 2) and 3) to apply the scheme to the multiple converters.

Proposed Current Control Scheme

Turning attention to quick current controllability of the second scheme, a current control scheme satisfying the foregoing requirements is proposed. Fig. 6 shows the basic principle of this scheme. The reference current is directly compared with the actual current. Then, the output signal of the comparator is sampled and held at a regular interval T_s synchronized with the clock of frequency equal to $1/T_s$. In the following experiments, T_s was set to 30 μs. Note that the 12 external clocks applied to each converter and to each phase in one converter do not overlap. Therefore, the harmonic currents are reduced considerably as if the switching frequency were increased.

EXPERIMENTAL RESULTS

Waveforms of p_L and q_L

The experimental compensation system is shown in Fig. 1. The load is a three-phase thyristor bridge converter of rating 20 kVA. Fig. 7 shows the experimental active power filter of rating 7 kVA. To discuss the compensation characteristics in the transient states, the firing angle of the thyristor bridge converter is controlled so as to generate the following dc output current:

$$i_d = I_d + I_{d0} \cdot \sin\ 2\pi f_0 \cdot t. \tag{11}$$

Then the harmonic frequencies f_h present in the input current are given by

$$f_h = f_i \pm nf_0 \qquad (6m \pm 1)f_i \pm nf_0 \tag{12}$$

where f_i is the line (input) frequency, $m = 1, 2, 3, \cdots$, and $n = 0, 1, 2, \cdots$. Fig. 8 shows the experimental frequency

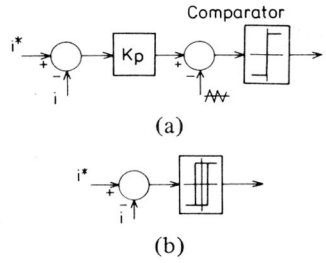

Fig. 5. Basic current control schemes. (a) Carrier signal. (b) Hysteresis comparator.

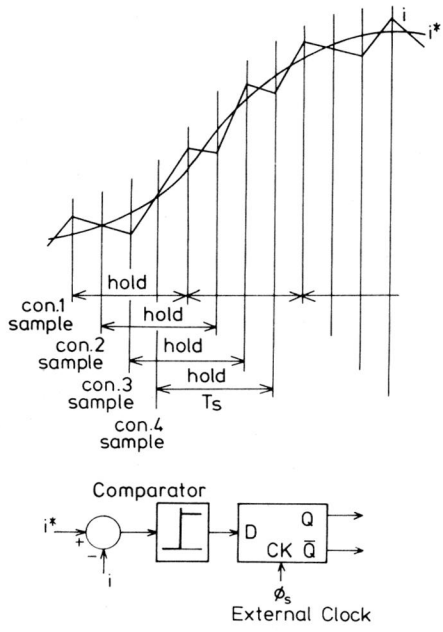

Fig. 6. Proposed current control scheme.

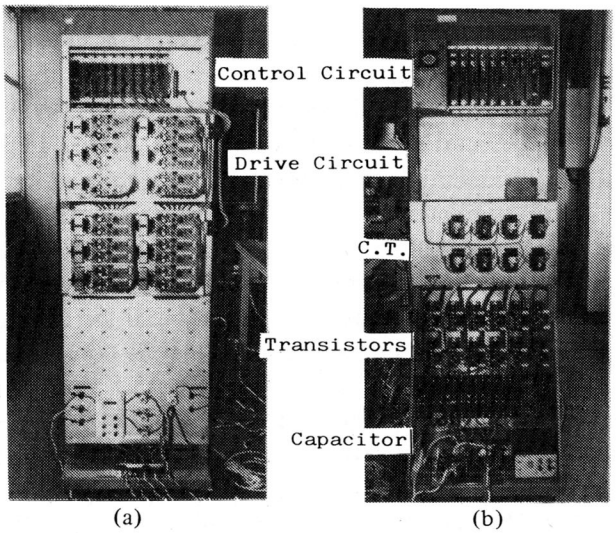

Fig. 7. Photograph of experimental active power filter. (a) Front. (b) Back.

spectrum around the line frequency under the following condition: line voltage (rms) = 200 V, f_i = 50 Hz, f_0 = 10 Hz, I_d = 50 A, I_{d0} = 30 A. The reason why f_0 was chosen as 10 Hz is that the frequency of the ''flicker'' caused by arc furnaces is about 10 Hz.

The experimental waveforms shown in Fig. 9 are the u-phase voltage e_u, the dc output current i_d, the u-phase input

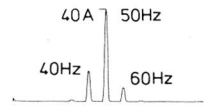

Fig. 8. Frequency spectrum of i_{Lu}.

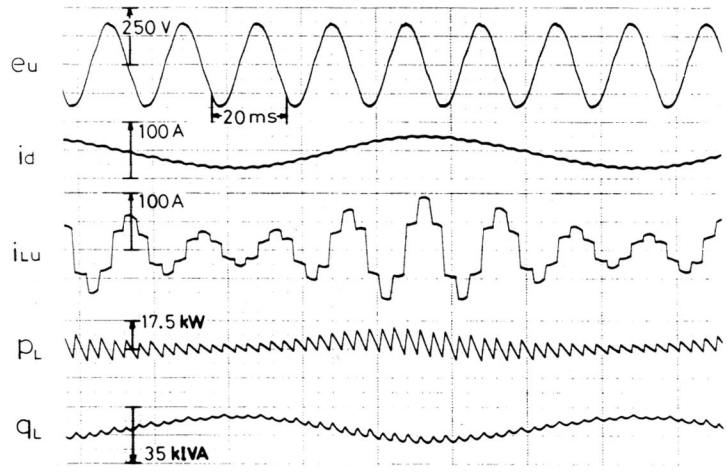

Fig. 9. Experimental waveforms.

current of the thyristor bridge converter, i.e., the u-phase load current i_{Lu}, and the instantaneous real and imaginary powers p_L and q_L under the same condition. The subharmonic current of 40 Hz and the superharmonic current of 60 Hz are caused by the component of 10 Hz present in $\tilde{p}_L$ and $\tilde{q}_L$. The amplitude of the sub- and superharmonic currents depends on the amplitude and phase of the component of 10 Hz in $\tilde{p}_L$ and $\tilde{q}_L$.

Compensation Characteristics

As shown in the previous section, the design of the low-pass filter in the calculation circuit of p^* and q^* has a significant effect on the compensation characteristics. In accordance with the compensation objectives, the Butterworth low-pass filter was designed as follows:

- *compensating condition a)*, i.e., when eliminating the harmonic currents of $5f_i \pm nf_0$, $7f_i \pm nf_0$, $\cdots$

  cutoff frequency = 150 Hz (fifth-order) for p^*,
  cutoff frequency = 150 Hz (fifth-order) for q^*;

- *compensating condition b)*, i.e., when eliminating the sub- and superharmonic currents related to $\tilde{q}_L$ around the fundamental and the harmonic currents of $5f_i \pm nf_0$, $7f_i \pm nf_0$, $\cdots$

  cutoff frequency = 150 Hz (fifth-order) for p^*,
  cutoff frequency = 0.9 Hz (second-order) for q^*;

- *compensating condition c)*, i.e., when eliminating all the harmonic currents of $f_i \pm nf_0$, $5f_i \pm nf_o$, $7f_i \pm nf_0$, $\cdots$

  cutoff frequency = 0.9 Hz (second-order) for p^*,
  cutoff frequency = 0.9 Hz (second-order) for q^*.

Fig. 10(a), (b), and (c) show the experimental compensation characteristics, corresponding to compensating conditions a),

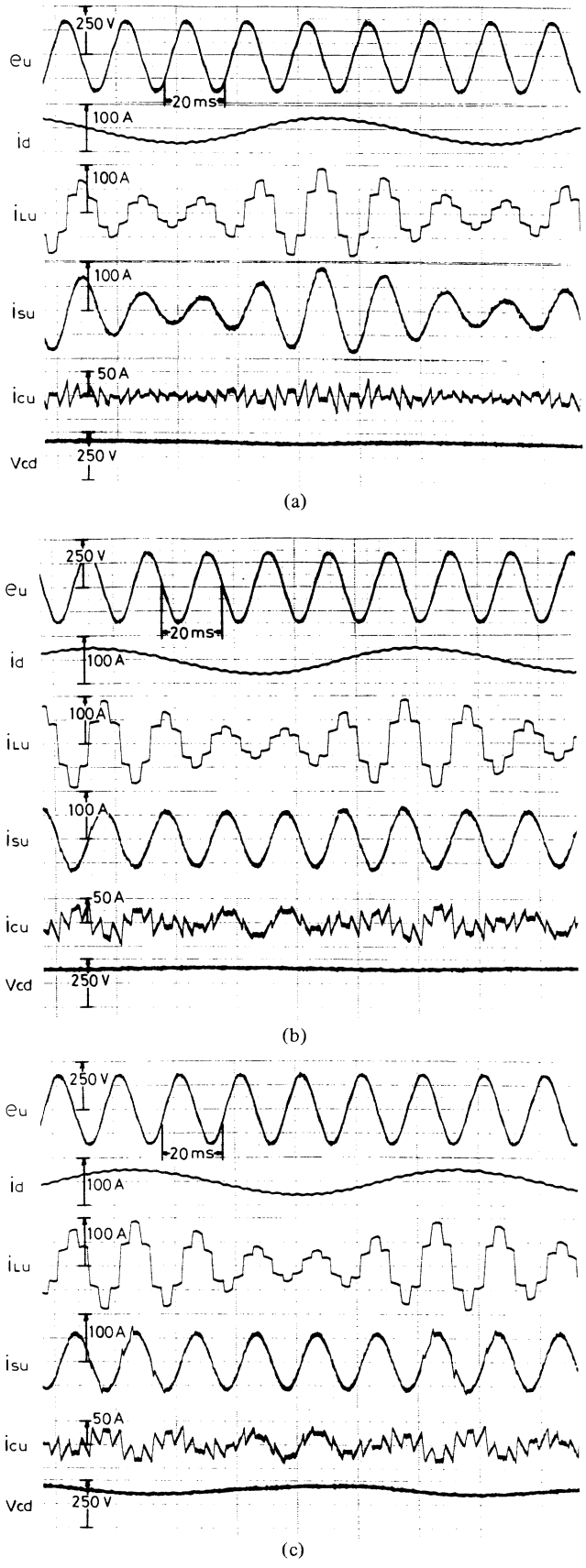

Fig. 10. Experimental compensation characteristics. (a) Condition a). (b) Condition b). (c) Condition c).

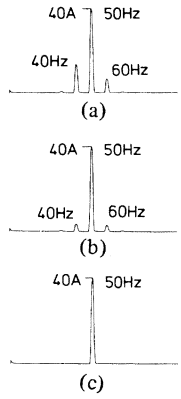

Fig. 11. Frequency spectrum of i_{Su}.

b), and c), respectively. Likewise, Fig. 11(a), (b), and (c) show the experimental frequency spectrum of i_{Su} around the fundamental frequency.

In compensating condition a), the harmonic currents having the frequencies of $5f_i \pm nf_0$, $7f_i \pm nf_0$, $\cdots$ are fully eliminated as shown in Fig. 10(a). On the other hand, the sub- and superharmonic currents around the fundamental are not eliminated at all, as shown in Fig. 11(a). However, this means that the experimental and theoretical compensation characteristics coincide under compensation condition a).

In Fig. 10(b) and (c), it is difficult to distinguish the compensation characteristics in compensating condition b) from those in compensating condition c) with respect to the waveform of i_{Su}. The sub- and superharmonic currents related to the component of 10 Hz present in $\tilde{p}_L$ exist in Fig. 11(b), while they are fully eliminated in Fig. 11(c). In Fig. 10(c), i_{Su} is sinusoidal and the amplitude is constant except for the intervals when the voltage across the dc capacitor drops below the reference voltage V^*_{Cd} (= 205 V). Note that the rms value of the subharmonic current of 40 Hz is equal to that of the superharmonic current of 60 Hz in compensating condition b).

The experimental results shown in Figs. 10 and 11 lead to the following essentials. To eliminate the sub- and superharmonic currents related to the component of 10 Hz present in $\tilde{p}_L$, the dc capacitor of the active power filter has to absorb the variation of the energy stored in the dc reactor of the thyristor bridge converter. This causes the variation of the dc capacitor voltage. Note that the dc capacitor voltage is constant in Fig. 10(b), while it varies at 10 Hz in Fig. 10(c). Accordingly, the active power filter which eliminates fully the sub- and superharmonic currents around the fundamental should be considered as the energy storage system, the purpose of which is to smooth the energy variation. Compensating condition b), therefore, is suitable for the active power filter using multiple voltage-source PWM converters, which is not realized by means of the conventional control strategy.

Conclusion

In this paper, the control strategy of the active power filter using multiple voltage-source PWM converters was proposed on the basis of the instantaneous reactive power theory. This was quite different from the conventional control strategy, thus succeeding in better compensation characteristics. The

cutoff frequency and order of the low-pass filter in the calculation circuit of p^* and q^* effected on the compensation characteristics in transient states. Thus various types of low-pass filters were designed, according to the compensation objectives. The better compensation characteristics were verified by experiments.

From the viewpoint of the initial and running cost, the active power filter is inferior to the passive power filter, i.e., the LC power filter at present. It is, however, most suitable to apply the active power filter to the suppression of the harmonic components present in the input current of large-capacity cycloconverters, because it is difficult for the passive power filter to eliminate their harmonic components having various frequencies.

REFERENCES

[1] B. M. Bird *et al.*, "Harmonic reduction in multiplex converters by triple frequency current injection," *Proc. Inst. Elec. Eng.*, vol. 116, p. 1730, 1969.

[2] H. Sasaki and T. Machida, "A new method to eliminate ac harmonic currents by magnetic flux compensation—Consideration on basic design," *IEEE Trans. Power App. Syst.*, vol. PAS-90, p. 2009, 1771.

[3] A. Ametani, "Harmonic reduction in thyristor converters by harmonic current injection," *IEEE Trans. Power App. Syst.*, vol. PAS-95, no. 2, 1976.

[4] N. Mohan *et al.*, "Active filters for ac harmonic suppression," presented at the IEEE/PES Winter Meeting, 1977, A77 026-8.

[5] I. Takahashi and A. Nabae, "Universal power distortion compensator of line commutated thyristor converters," in *Proc. IEEE/IAS Annual Meeting*, 1980, p. 858.

[6] L. Gyugyi and E. C. Strycula, "Active ac power filters," in *Proc. IEEE/IAS Annual Meeting*, 1976, p. 529.

[7] H. Kawahira, T. Nakamura, and S. Nakazawa, "Active power filters," in *Proc. JIEE IPEC-Tokyo*, 1983, p. 981.

[8] K. Hayafune *et al.*, "Microcomputer controlled active power filters," in *Proc. IEEE/IES IECON*, 1984, p. 1221.

[9] H. Akagi, Y. Kanazawa, and A. Nabae, "Instantaneous reactive power compensators comprising switching devices without energy storage components," *IEEE Trans. Ind. Appl.*, vol. IA-20, p. 625, 1984.

[10] B. R. Pelly, *Thyristor Phase-Controlled Converters and Cycloconverters.* New York: Wiley, 1971.

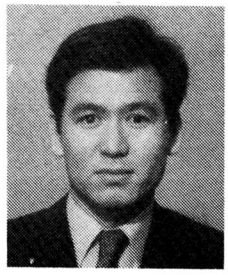

Hirofumi Akagi was born in Okayama Prefecture, Japan, on August 19, 1951. He received the B.S. degree from the Nagoya Institute of Technology, Nagoya, Japan, in 1974 and the M.S. and Ph.D. degrees from the Tokyo Institute of Technology, Tokyo, Japan, in 1976 and 1979, respectively, all in electrical engineering.

Since 1984, he has been an Associate Professor at the Technological University of Nagaoka, Japan. He is engaged in research on ac motor drives, active power filters, and high-frequency inverters.

Dr. Akagi is a member of the Institute of Electrical Engineers of Japan.

Akira Nabae (M'79) was born in Ehime Prefecture, Japan, on September 13, 1924. He received the B.S. degree from Tokyo University, Tokyo, Japan, in 1947, and the Dr.Eng. degree from Wasada University, Japan.

He joined Toshiba Corporation in 1951. From 1951 to 1970, he was engaged in the research and development of rectifier and inverter technology at Tsurumi Works Engineering Department. From 1970 to 1978, he was involved in research and development of power electronics, especially ac drive systems at the Heavy Apparatus Engineering Laboratory. Also, from 1972 to 1978, he was a nonoccupied Lecturer of Wasada University, Japan. Since 1978, he has been a Professor at the Technological University of Nagaoka, Japan. He is now interested in energy conversion and control systems.

Dr. Nabae is a member of the Institute of Electrical Engineers of Japan.

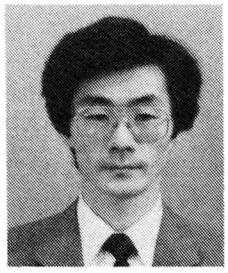

Satoshi Atoh was born in Nagano Prefecture, Japan, on August 26, 1960. He received the B.S. and M.S. degrees in electrical engineering from the Technological University of Nagaoka, Japan, in 1983 and 1985, respectively.

In 1985 he joined Toyo Electric Manufacturing Company, Ltd. He is now engaged in research on active power filters.

Mr. Atoh is a member of the Institute of Electrical Engineers of Japan.